journal

J. Am. Ceram. Soc., 75 [5] 1108-16 (1992)

Cubic-to-Tetragonal (t') Transformation in Zirconia-Containing Systems

Tzer-Shin Sheu,* Tseng-Ying Tien,* and I-Wei Chen*

Department of Materials Science and Engineering, University of Michigan, Ann Arbor, Michigan 48109-2136

The coexistence of the cubic fluorite and tetragonal phases in rapidly quenched samples was studied in the ZrO_2–$MO_{1.5}$ systems for M = Sc, In, Y, and rare earths (R). Spontaneous transformation from metastable cubic phase was triggered at room temperature by a mechanical force. Isolated tetragonal platelets in the cubic matrix were bounded by {101} habit planes and contained anti-phase boundaries. The tetragonality decreased with stabilizer content and vanished at around 18 mol% for M = Y and R, 23 mol% for M = Sc, and 25 mol% for M = In, all at room temperature. With increasing temperature, the tetragonality initially increased because of anisotropic thermal expansion, then decreased rapidly, after reaching a maximum, as the temperature for the tetragonal-to-cubic transformation was approached. Being a first-order martensitic transformation, the cubic-to-tetragonal transformation is accompanied by a discontinuous change of tetragonality and a hysteresis loop as the temperature or composition passes through the equilibrium value. [Key words: zirconia, transformations, microstructure, phase diagrams, quenching.]

I. Introduction

A RAPID phase transformation from a cubic (c) to a tetragonal symmetry in the ZrO_2–$YO_{1.5}$ system was first reported by Scott in 1975.[1] This tetragonal phase was later found to be different from the regular tetragonal phase that existed in most of the zirconia systems. Notably, it had a smaller tetragonality, a higher yttrium content, many anti-phase domain boundaries (APB) never seen in the regular tetragonal phase, and a higher stability against further distortion into the monoclinic symmetry.[2-12] Following Miller *et al.*,[2] this phase has been termed t' phase to distinguish it from the regular tetragonal t phase. Lanteri *et al.* later emphasized that the t' phase was not an equilibrium phase,[5,10-12] in contrast to the t phase which formed from the c phase by precipitation.[4]

Recently this cubic-to-tetragonal transformation was observed in a number of zirconia–rare-earth oxide ($RO_{1.5}$) systems prepared by rapid melt quenching.[13] The tetragonality in these systems followed a unique compositional dependence regardless of the trivalent stabilizing dopant oxides used. Similar results had been reported by Lefevre in 1963.[14] The upper limit of the stabilizing oxide concentration at which the tetragonal phase could be observed was 14.0 mol% $RO_{1.5}$ in Yoshimura's report[13] and ~18 mol% $RO_{1.5}$ in Lefevre's report.[14] It should also be noted that the lattice parameters in the cubic and the tetragonal zirconia solid solutions generally correlate well with the ionic radius and the charge of the stabilizer cation.[15] For example, the lattice parameters of both the cubic and tetragonal zirconia phases increase with the stabilizer concentration in the ZrO_2–$RO_{1.5}$ systems (except R = Lu),[13,14] remain constant in the ZrO_2–$InO_{1.5}$ system,[16] and decrease in the ZrO_2–$ScO_{1.5}$ system.[17]

Regarding the nature of the c-to-t' phase transformation, there have been various and sometimes contradictory suggestions. The transformation has been described as displacive,[5,6,10-12] diffusionless,[5,6,10-12] first order,[11] second order,[18] martensitic,[6] nonmartensitic,[5,11,12] massive,[5] homogeneous,[5,11] and heterogeneous.[6] For example, Heuer and co-workers believe that the c-to-t' transformation in ZrO_2–$YO_{1.5}$ alloys is first order, diffusionless, displacive but nonmartensitic, and that it is homogeneously nucleated, with a non-glissile interface, and growth-controlled by heat transfer.[11] The controversy partly stems from the fact that the transformation occurred at very high temperatures and that the remnant microstructures observed at room temperature did not usually contain any cubic phase. Thus, the coexistence of the cubic and t' phases has not been commonly achieved in the laboratory,[6,10,12] making it difficult to examine the progress of the transformation and the attendant morphological characteristics such as habit planes in order to ascertain the nature of the transformation.

With different trends for lattice parameter changes in the ZrO_2–$MO_{1.5}$ systems in mind, we have systematically studied the c-to-t' transformation for M = Y, Yb, In, and Sc. We have found that the c-to-t' transformation can be triggered at ambient temperature and that the coexistance of the c and t' phases in some cases is possible. Special emphasis has also been placed on the temperature dependence of the tetragonal distortion in order to gain a better insight into the nature of the transformation. These results are reported below.

II. Experimental Procedure

Starting materials used were 99.9% pure $MO_{1.5}$ (M = Y, Yb, In, and Sc) and 93.1% pure $ZrOCl_2 \cdot 8H_2O$ oxides. $MO_{1.5}$ was dissolved in a hot HCl solution and the $ZrOCl_2 \cdot 8H_2O$ was dissolved in distilled water. A solution of NH_4OH (10 wt%) and a mixture of MCl_3 and $ZrOCl_2$ solutions were simultaneously added to a beaker to form gel-like hydroxide precipitates by controlling the pH value above 9. After filtration, the precipitates were dried in an oven at 80°C. Dried precipitates were calcined in an air furnace at 650°C for 2 h. Pellets were formed under a uniaxial pressure and then isostatically pressed at 350 MPa.

Pellets were sintered and heat-treated in an arc-melting unit or air furnace with $MoSi_2$ heating elements, then water quenched. Phase analysis was performed by X-ray diffraction using a Rigaku diffractometer equipped with a high-temperature camera and a rotating anode X-ray source for Cu$K\alpha$ radiation. Microstructures were examined by transmission electron microscopy using a JEOL 2000 FX microscope operating at 200 kV and scanning electron microscopy using several microscopes.

A. Virkar—contributing editor

Manuscript No. 196808. Received April 2, 1991; approved 1/10/92.
Supported by the U.S. National Science Foundation under Grant No. DMR-8807024 and by the University of Michigan.
*Member, American Ceramic Society.

III. Results and Discussion

(1) Microstructure and Coexistence of c and t' Phases

Some SEM micrographs of representative microstructures of the t' phase in the ZrO_2–$MO_{1.5}$ (M = Sc, In, Y) are presented in Fig. 1. Their morphology is similar in all the systems studied and contains closely spaced twin platelets of certain crystallographic orientations. In most cases, more than one twin orientation, including sometimes the so-called "herringbone" structure,[9] are present within a single grain. Some variants apparently intersect each other, as can be seen from the SEM micrograph shown in Fig. 2. The above features are characteristic of phase transformations involving lattice distortion, both for martensitic transformations and for diffusion-controlled phase precipitations. The twins could come either from the c-to-t' transformation itself, as incorporated in the so-called "lattice invariant deformation" (LID) operation during the transformation,[19] or from the mechanical accommodation of the product t' phase subsequent to the transformation. This distinction cannot be ascertained by mere examination of the final microstructure.[20] Indeed, from a phenomenological, crystallographic viewpoint, it can be readily predicted that the cubic-to-tetragonal transformation will most likely entail $\{011\}\langle 0\bar{1}1\rangle$ twinning systems in the microstructure to minimize the distortional energy.[20,21] Such an analysis has been performed by Kato and co-workers for zirconia systems, which explains the experimental observations very well.[20,22]

We have made a special effort to investigate whether the c-to-t' transformation can be triggered at room temperature and, if so, whether the microstructure can be preserved to reveal the coexistence of the c and t' phases. Some of the successful attempts are described below. In one case, a quenched specimen containing 14.0 mol% $ScO_{1.5}$ was first identified to be essentially cubic by X-ray diffraction. It was then mechanically polished in order to induce the c-to-t' transformation. In Fig. 3 we show the X-ray diffraction patterns before and after polishing. The as-quenched sample gives rise to only cubic reflections; after polishing, the coexistence of tetragonal reflections becomes prominent as readily seen from the splitting of the (113) and the (202) peaks and the broadening of the (222) peak. A set of SEM micrographs of this sample, before and after polishing, are presented in Fig. 4. They illustrate a substantial increase of the platelike t' variants due to polishing and provide direct evidence that the transformation is a martensitic one. The coexistence of the cubic and the t' phases was further verified by TEM using thin foil samples of the same compositions subject to a similar quenching heat treatment. The electron diffraction pattern shown in Fig. 5(a) reveals both the cubic and the tetragonal reflections of one variant. This tetragonal variant forms iso-

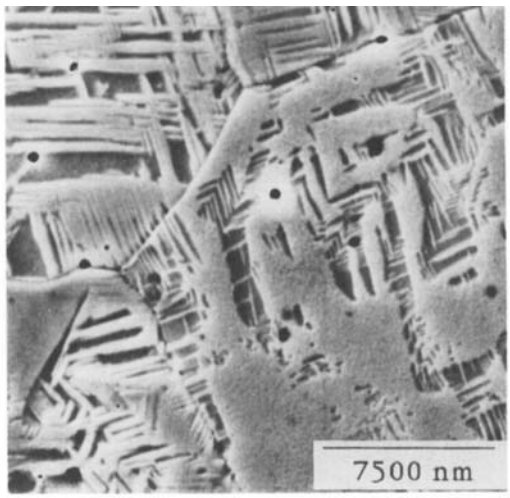

(a)

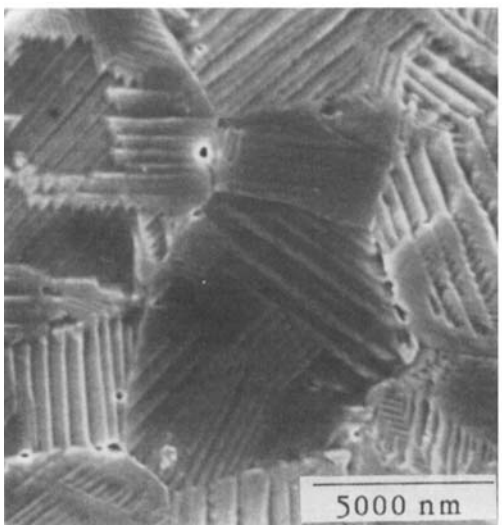

(b)

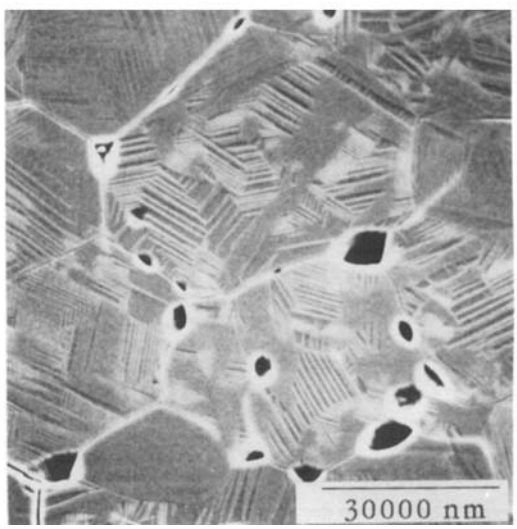

(c)

Fig. 1. Microstructures of t' phase in ZrO_2–$MO_{1.5}$ systems: (a) 12.0 mol% $ScO_{1.5}$, (b) 14.8 mol% $InO_{1.5}$, (c) 12.5 mol% $YO_{1.5}$.

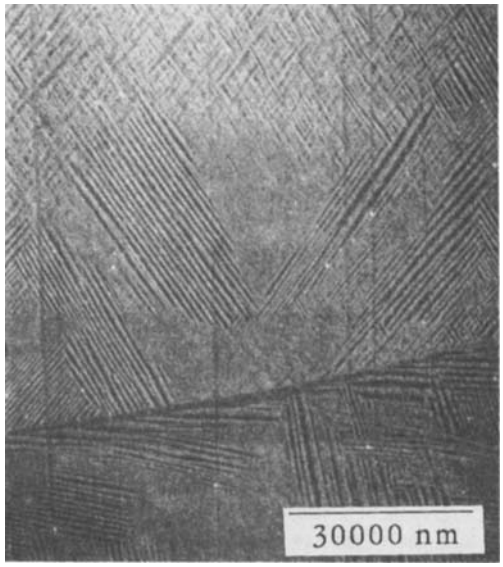

Fig. 2. A 6.0 mol% Y_2O_3 arc-melted sample containing several orientations of t' phase.

lated platelets in Fig. 5(b) under bright field and Fig. 5(c) under dark field. From a trace analysis, the habit plane of the t' phase was found to lie along the {101} planes which are expected for the cubic-to-tetragonal transformation.[20,21]

In addition to the above example, the coexistence of the cubic and the t' phases was also observed in a 14.0 mol% $YO_{1.5}$ sample, as shown in Fig. 6. A TEM study with imaging through ⟨112⟩ reflections with a [111] zone axis in another 14.4 mol% $YO_{1.5}$ sample has also been conducted. As described in the Appendix, the latter result unequivocally confirms that the cubic phase can coexist with tetragonal variants at room temperature.

The dark-field image in Fig. 5(c), taken using the characteristic tetragonal diffraction spot {112}, shows within the t' plates features which are reminiscent of the APB described by other workers[3-5,7,8,10-12] for $YO_{1.5}$-containing zirconia transforming at higher temperatures. Their presence in the room-temperature-transformed specimens strongly suggests that the mechanically induced c-to-t' transformation at room temperature is probably of the same nature as those occurring at higher temperatures or during cooling, as extensively reported by other investigators.[2-12] Specifically, we believe that in all cases, the c-to-t' transformation proceeds martensitically, beginning with one variant, followed by other variants, and twins necessitated by strain-accommodation considerations, especially if motivated by an increasing driving force as during subsequent cooling.

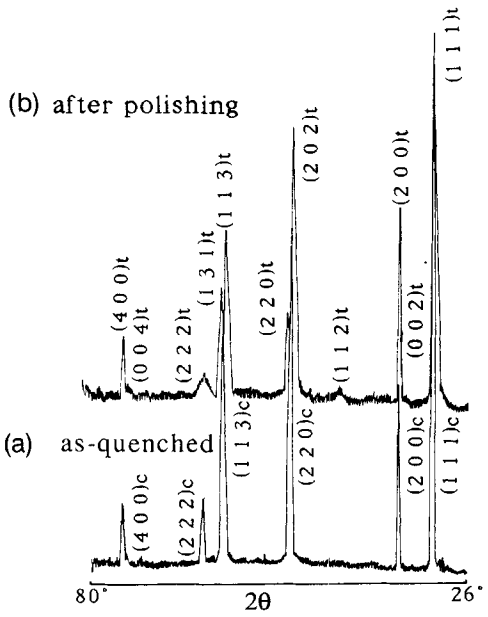

Fig. 3. X-ray diffraction pattern of a 14.0 mol% sample (a) before and (b) after mechanical polishing.

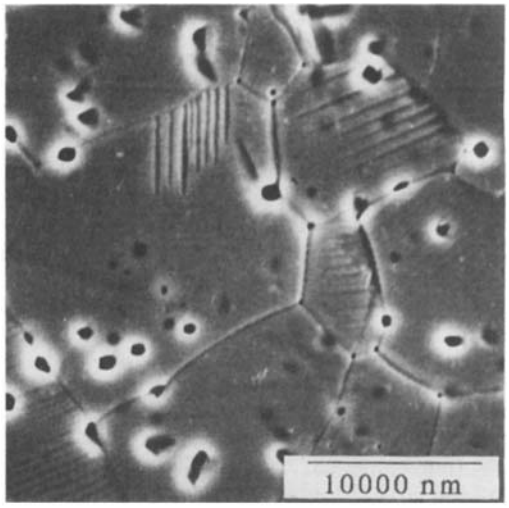

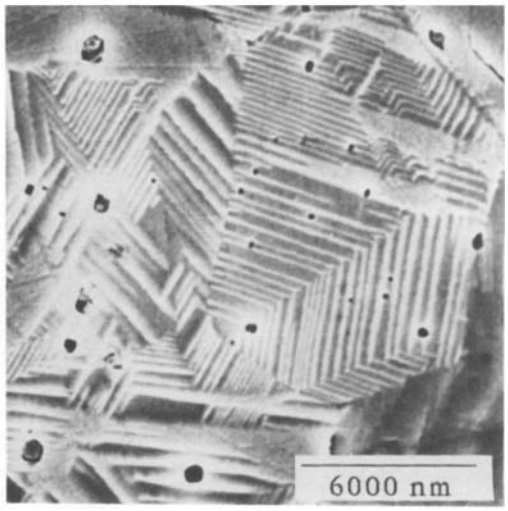

Fig. 4. Morphology of t' phase in a 14.0 mol% $ScO_{1.5}$ sample (a) before and (b) after mechanical polishing.

Finally, the existence of single-variant tetragonal platelets within a cubic matrix implies some incomplete strain energy relief during martensitic transformation. Anti-phase domains are theoretically of the same crystallographic orientation and not capable of self-accommodation commonly ascribed to other LID such as twins. This situation is not unusual, however, for zirconia transformation. Indeed, both for the nucleation of the tetragonal-to-monoclinic transformation,[23] and for the growth of the orthorhombic-to-monoclinic transformation[24] coherent, single-variant habit relationships between the parent and product phases have already been established in this ceramic.

(2) Compositional Dependence of Tetragonal Distortion

Lattice parameters at room temperature in various ZrO_2–$MO_{1.5}$ systems are presented in Fig. 7. The unit-cell volumes of the cubic and the tetragonal phases are plotted in Fig. 8. By comparison, the results of the ZrO_2–$YO_{1.5}$ and ZrO_2–$YbO_{1.5}$

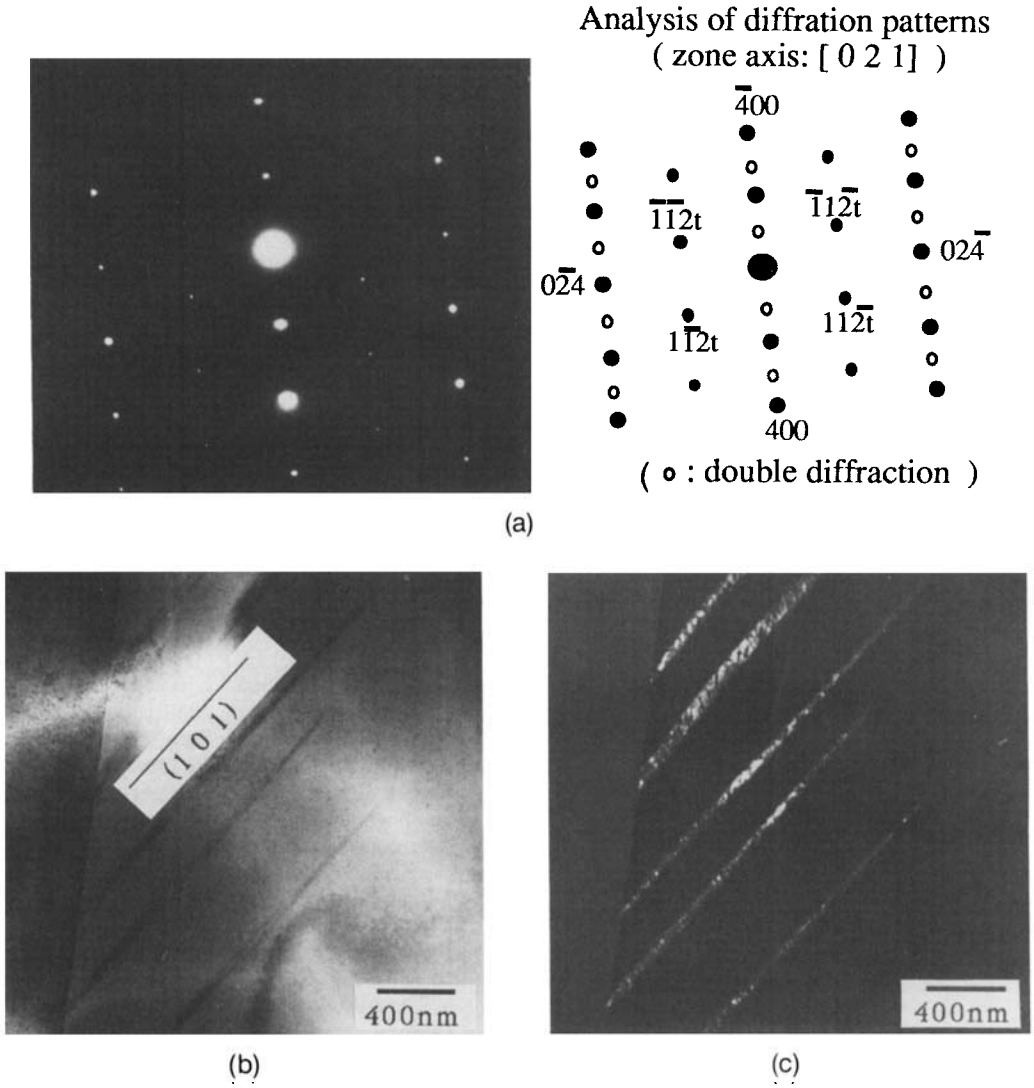

Fig. 5. TEM micrographs of a 14.0 mol% $ScO_{1.5}$ sample containing cubic and t' phases: (a) selected area diffraction pattern showing c and t' reflections; (b) tetragonal variant (bright field) showing {101} habit planes; (c) same variant (dark field from (112)) showing anti-phase boundaries inside t'.

systems are found very close to those reported by Lefevre,[13] Scott,[1] and Yoshimura[14] for $YO_{1.5}$- and $RO_{1.5}$-containing zirconia. We note that the lattice parameters of the tetragonal cell in Fig. 7 can be extrapolated to intersect at a point which apparently coincides with the lattice parameter of the cubic phase of the corresponding composition. This is complemented by the observation in Fig. 8 of a common straight line correlation of the tetragonal and the cubic unit-cell volumes. These features can be understood if we accept the notion that the c-to-t' transformation involves pure shear and no dilatation. It should also be noted that at low concentrations, the extropolated tetragonal distortion of the t' phase agrees with that of the t phase. Thus, from a crystallographic point of view, the t' phase is apparently the extension of the t phase and not a distinct new structure. Lastly, some of the cubic phase data fall within the "wedge" bounded by the tetragonal lattice parameters. For such compositions, a tetragonal distortion of the cubic phase is theoretically possible. Similar findings have been reported by Scott[1] and Yoshimura.[14]

For M = Y and rare earths, Lefevre[13] and Yoshimura[14] have observed that the compositional dependence of the tetragonality follows a unique relation which is independent of M. To examine whether this relation applies to M = Sc and In, we plot the tetragonality of all the systems in Fig. 9 (lower half). It then becomes clear that the decrease of tetragonality for a given amount of $InO_{1.5}$ is less than that for $ScO_{1.5}$, which is in turn less than that for $YO_{1.5}$ or $RO_{1.5}$. This point can be made even clearer if we reduce Fig. 7 into a normalized plot, Fig. 9 (upper half), by subtracting a reference lattice constant, a^*, defined as the extropolated cubic lattice parameter at the same composition, from the tetragonal lattice parameters (a, c). The intersect of the a–a^* and c–c^* lines for M = Y and R is around 18 mol%, for M = Sc around 23 mol%, and for M = In around 25 mol%. Thus, the unique relation for ZrO_2–$(Y, R)O_{1.5}$ systems cannot be generalized to ZrO_2-$ScO_{1.5}$ and ZrO_2–$InO_{1.5}$ systems.

(3) Temperature Dependence of Tetragonal Distortion

The as-quenched tetragonal phase was reheated to higher temperatures to study the reverse t'-to-c transformation. Figure 10 shows the tetragonality as a function of temperature of the 14.8 mol% $ScO_{1.5}$ sample. As temperature increases, the tetragonality rises to a maximum at around 250°C, then decreases and vanishes above 800°C. In this study, splitting of the {400} peaks was used as the main indicator for identifying the t' and the c phase. With the overlapping $(400)_t$ and $(004)_t$ peaks at higher temperatures, a tetragonality of less than 1.001 was difficult to ascertain within the experimental resolution of high-temperature X-ray diffractometry. This was the case in Fig. 10 between 750° and 850°C, above which a single $(400)_c$ peak was present. Similar tetragonality curves were obtained for the ZrO_2–$YO_{1.5}$ system for several compositions,

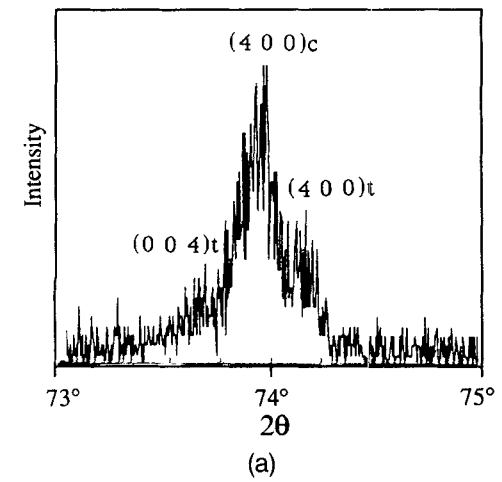

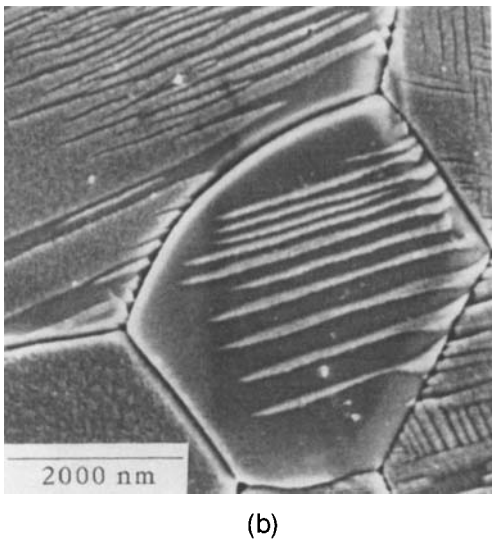

Fig. 6. (a) X-ray diffraction pattern and (b) SEM micrograph of a 14.0 mol% $YO_{1.5}$ sample containing cubic and t' phases.

shown in Fig. 11, with the feature of the tetragonality maximum highlighted in the inset for one composition. Also included are the data for pure ZrO_2 between 1100° and 2400°C, reported by Aldebert *et al.*,[25] which are complemented by the tetragonality of pure ZrO_2 at room temperature, placed at

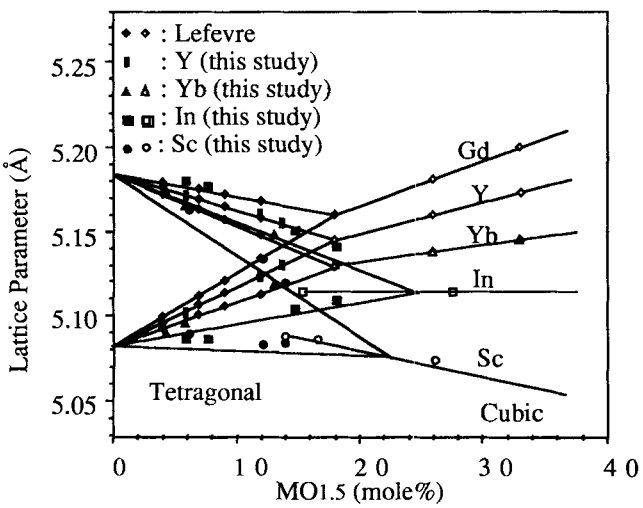

Fig. 7. Lattice parameters of four ZrO_2–$MO_{1.5}$ systems at room temperature. Filled symbols for tetragonal and open symbols for cubic.

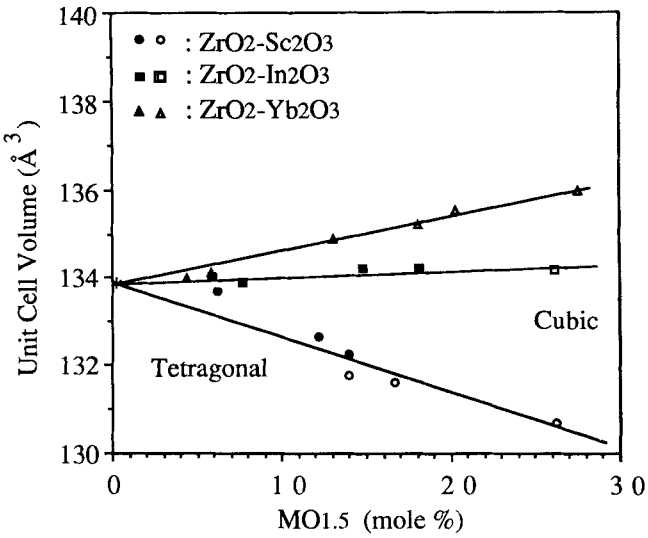

Fig. 8. Unit-cell volumes of cubic and tetragonal phases of three ZrO_2–$MO_{1.5}$ systems. Filled symbols for tetragonal and open symbols for cubic.

1.020, taken from Fig. 9 (see symbol "*"). It is clear that as the yttria content increases, the tetragonality decreases and the maximum on the tetragonality curve shifts to a lower temperature. As before, these data can be normalized using a^* and replotted in Fig. 12 as a function of $YO_{1.5}$ composition. At higher temperatures, the onset of tetragonality is higher at a small stabilizer content but it also decreases faster as the stabilizer content increases. Indeed, as already seen in Fig. 11, the pure zirconia which undergoes the c-to-t' transition at 2300°C has a maximum tetragonality of around 1.025 at about 1700°C. This is the highest tetragonality (the largest normalized a and the smallest normalized c) of any zirconia system and is indicated in Fig. 12 by a set of arrows.

The initial increase of the tetragonality is a consequence of thermal expansion which is higher along the c axis than along the a axis. This result can be intuitively understood as due to the different bond strengths in the c and a axes, with the longer axis having a weaker bond. Despite the thermal expansion anisotrophy, the tetragonality eventually decreases as the

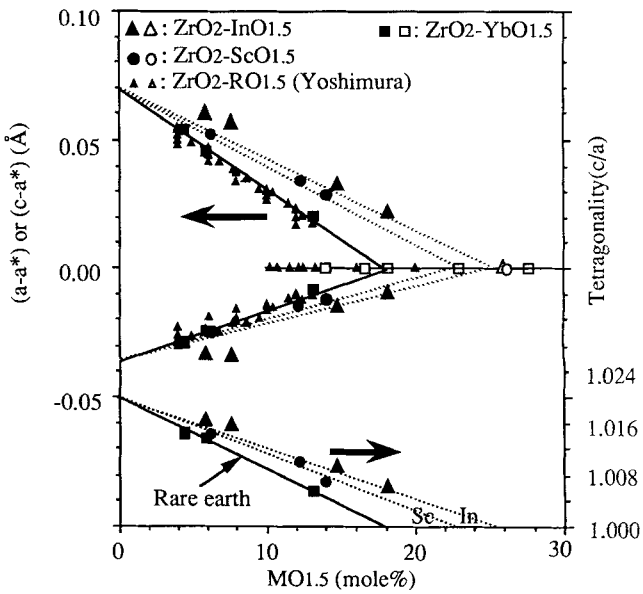

Fig. 9. Normalized lattice parameters and tetragonality of four ZrO_2–$MO_{1.5}$. a^* is the measured or the extrapolated cubic lattice parameter at the composition. Data of $RO_{1.5}$ taken from Ref. 14.

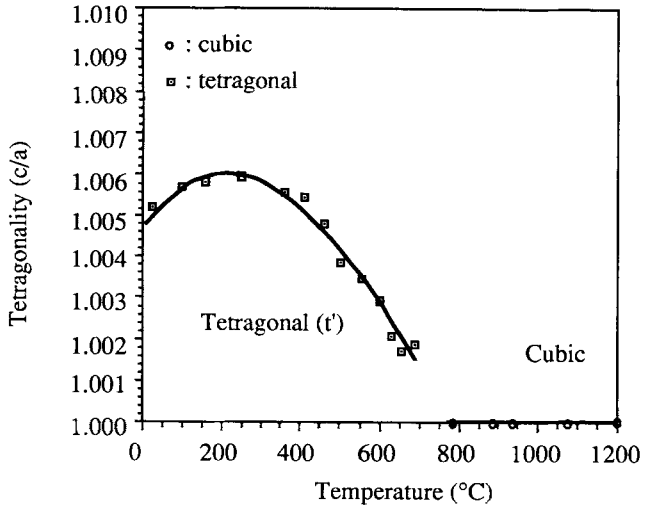

Fig. 10. Tetragonality as a function of temperature in a 14.8 mol% $ScO_{1.5}$ sample.

t'-to-c transformation temperature, which decreases with increasing stabilizer contents, approaches.

Finally, as mentioned previously, the c-to-t' transformation involves only pure shear and no dilatation. This was also verified for the reverse t'-to-c transformation. Specifically, dilatometry curves were obtained for a 13.5 mol% $YO_{1.5}$ sample heated to 1000°C; no discontinuous dimensional change was detected.

IV. Implications

The observation of the spontaneous, shear-dominant c-to-t' transformation at room temperature, induced by a mechanical force, unambiguously identifies the transformation as a martensitic one. It proceeds with a characteristic (101) habit plane which is generally expected for the cubic-to-tetragonal transformation. It also imparts all the microstructural features of the c-to-t' transformation reported in the literature, including the appearance of single and multiple twins and APB in the t' platelets. Based on the observation of the single variant t' platelet bounded by (101) habit planes, we can conclude that those twins visible in Fig. 1 are not LID transformation twins but rather mechanical twins which form

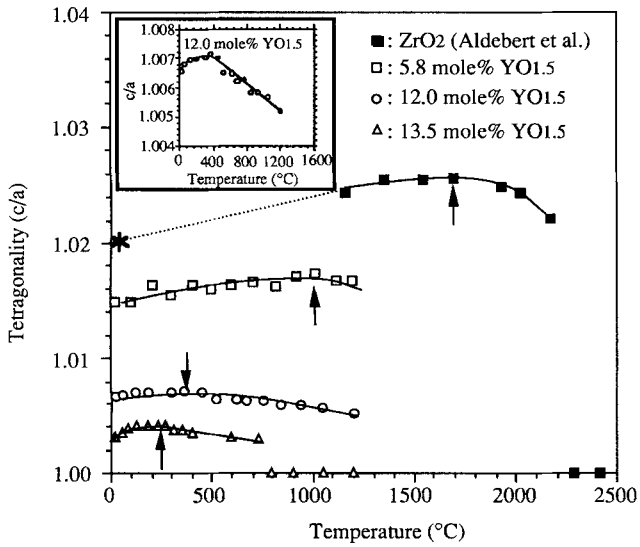

Fig. 11. Tetragonality vs temperature in ZrO_2–$YO_{1.5}$ system. Arrows indicate locations of tetragonality maxima, one of them highlighted in the inset. Data of pure zirconia at high temperatures taken from Ref. 23.

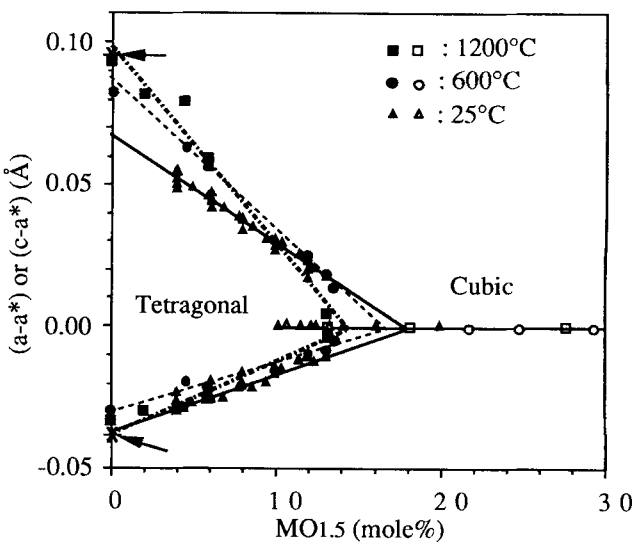

Fig. 12. Normalized lattice parameters at three temperatures of ZrO_2–$(Y,Yb)O_{1.5}$ systems. Full symbols for tetragonal and open symbols for cubic. Arrows indicate lattice parameters of pure zirconia at its peak tetragonality near 1700°C.

substantially subsequent to the transformation to minimize the strain energy.[12] As elucidated by Michel *et al.*[3] and Heuer *et al.*,[4,5,8,10,11] the two types of t' domains (bounded by APB) are due to symmetry breaking into the c-to-t' transformation of the fluorite structure and are of the same lattice correspondence to the parent c phase. Thus, they are analogous to the two spin states in the magnetic transition (describable by the so-called Ising model[24]) which need not cause any crystallographic distortion. Hence, they are of no consequence for the consideration of the martensitic transformation.

The martensitic transformation is a first-order type since it involves a hysteresis, as exemplified by the existence of the metastable cubic state, at room temperature. An order parameter[26] can now be defined, $\eta = (c - a)/a$, to describe the transformation. At equilibrium, the order parameter undergoes a discontinuous change for a first-order transformation. Kinetic considerations further dictate that a hysteresis loop spanning above and below the equilibrium point accompanies such a phase change. In this regard, the extension of the cubic phase somewhere into the tetragonal "wedge" of Figs. 7 and 9 is unavoidable—otherwise it would be a second-order phase transformation. For the same reason, as the temperature increases, the tetragonality must experience a discontinuous drop to unity at a certain temperature, even though the high-temperature data of Figs. 10 and 11 are not sufficiently refined to manifest this discontinuity more clearly.

To elucidate the above point further, the relationships between the free energy diagram, phase diagram, and the tetragonality or order parameter, with their composition and temperature dependence are schematically illustrated in Figs. 13 and 14 for the zirconia alloys. Here, we will use two separate free energy curves for the tetragonal and the cubic phases, respectively, which is appropriate for the first-order phase transformation. In Fig. 13(a), the free energy diagram is represented as a function of composition. The composition where the two branches meet is denoted by X_0, and the two equilibrium compositions determined by the common tangent are denoted by X_1 and X_2. As pointed out by Heuer *et al.*,[4,5,10,12] a displacive c-to-t' transformation can occur in any supercooled composition less than X_0. Alternatively, if an arbitrary tetragonal distortion, such as the one recently discussed by Negita,[26] is introduced to the cubic phase of a fixed composition, the free energy may be traced schematically as a function of order parameter by adopting a phenomenological Ginzburg–Landau type of description.[27,28] This is illustrated in Fig. 13(b) for a first-order transformation. The locus along the local

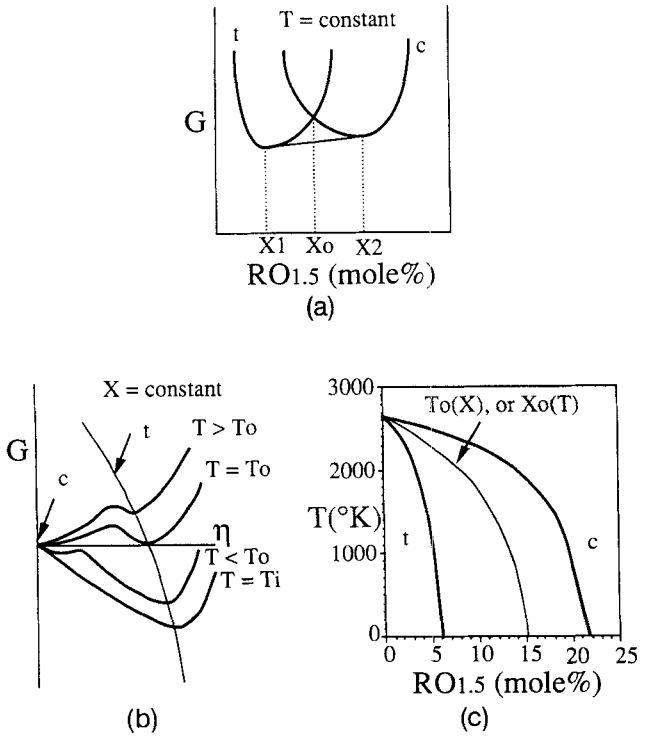

Fig. 13. Free energy as a function of (a) composition and (b) order parameter and temperature. Also shown in (c) is a ZrO_2–$RO_{1.5}$ phase diagram.

minima at a non-zero-order parameter corresponds to the tetragonal branch; the cubic branch corresponds to the origin. At T_0, the two have the same free energy, whereas above T_0, the cubic branch has a lower energy. Note that even below T_0, an energy barrier exists between the metastable cubic phase and the stable tetragonal phase. Thus, martensitic transformation under such conditions is still most likely controlled by heterogeneous nucleation.[23,29–31] However, along the lowest branch of Fig. 13(c), labeled $T = T_i$, the cubic lattice is so unstable that there is no energy barrier for the tetragonal distortion. Theoretically, this case can be realized if heterogeneous nucleation is suppressed and the material is supercooled to near instability. Then the transformation may become homogeneous and proceed with a diffuse interface.[29–31] In reality, however, this does not seem to be the case for the *c*-to-*t'* transformation, at least at temperatures as low as room temperature, since a sharp interface was still observed there (Fig. 5). We therefore conclude that the martensitic transformation we observed is also triggered by heterogeneous nucleation. A schematic phase diagram consistent with these free energy diagrams is shown in Fig. 13(d), in which X_0 and T_0 are indicated.

Referring to the above diagrams, the order parameter is now schematically plotted as a function of composition in Fig. 14(a), and of temperature in Fig. 14(b), for a first-order displacive transformation. Also indicated are a set of hysteresis loops, although their widths are kinetically determined and not known a priori. (The equilibrium compositions, X_1 and X_2 in Fig. 13(a), of the two-phase field always lie somewhere outside the hysteresis loop for the martensitic transformation, and their attainment will ultimately require diffusion.) The combined effects of temperature, composition, and anisotropic thermal expansion are illustrated in Figs. 14(c) and (d), by analogy with Figs. 11 and 12. The crossover of $\eta(X)$ lines of different temperatures is entirely the result of anisotropic thermal expansion. For a given composition, say X^*, it can be verified in Fig. 14(c) that as the temperature increases, the tetragonality initially increases (T_a to T_b) but later decreases (T_b to T_c). Alternatively, for a given temperature range, say between T_b and T_c, as the composition increases, the tetragonality initially increases with temperature ($X < X^{**}$) but later decreases with temperature ($X > X^{**}$). These features are also evident in Fig. 14(d). Together, these schematic diagrams summarize from a phenomenological viewpoint our experimental results and the basic thermodynamic and crystallographic features of the cubic and tetragonal phases.

One additional observation of our study is of interest from a crystal chemistry viewpoint. For $YO_{1.5}$- and $RO_{1.5}$-containing zirconia, the composition when η extrapolates to zero can be placed at around 19 mol% at 0 K. Ho has used a simple model based on the consideration of coordination number to arrive at an estimation of 20 mol% as that required for stabilizing the cubic phase.[32] The data for $YO_{1.5}$ and $RO_{1.5}$ are consistent with his model. However, $ScO_{1.5}$ and $InO_{1.5}$ apparently are not as effective for stabilization as $YO_{1.5}$ and $RO_{1.5}$ and their required composition to reduce η to zero (by extrapolation) is definitely above 20 mol%. This difference might be due to their smaller ionic radii and/or different types of bonding as compared to those of $YO_{1.5}$ and $RO_{1.5}$ in zirconia. We should

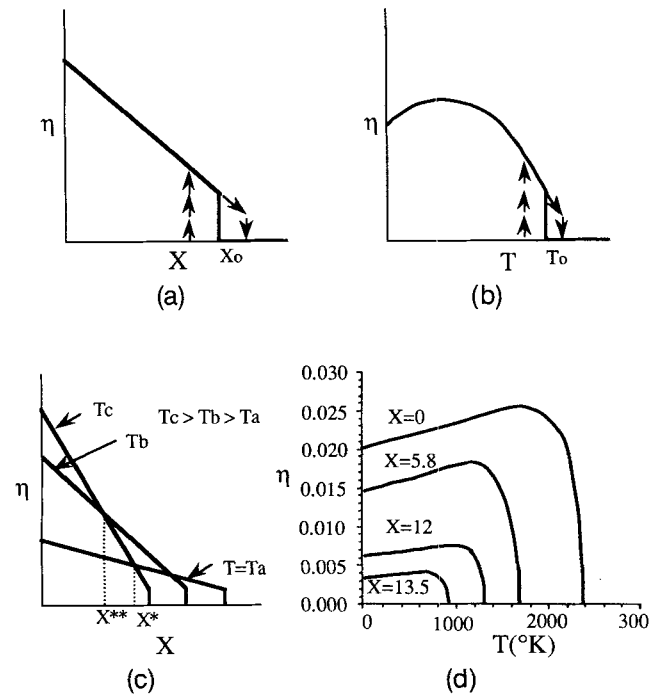

Fig. 14. Order parameter as a function of (a) composition, (b) temperature, and (c, d) both.

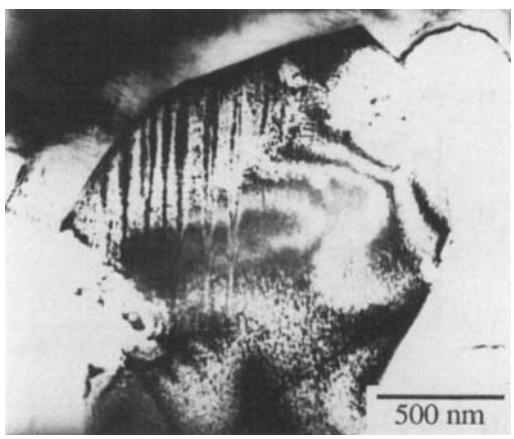

Fig. A1. TEM micrograph showing *t'* phase grown from the grain boundary and then terminated inside the grain.

note, however, that the thermodynamic equilibrium usually does not coincide with $\eta = 0$ in first-order transformations. This feature is already illustrated in Figs. 14(a) to (d).

Lastly, although the t' phase is usually very resistant to the tetragonal-to-monoclinic transformation, we did occasionally evidence such transformation after mechanical polishing in our study. Similar marginally transformable t' phases were also found in a 4.6 mol% CaO stabilized ZrO_2 and a 6.0 mol% MgO stabilized ZrO_2.[33] Recent results of Virkar and co-workers further discovered that, as the twin boundaries were removed by mechanical poling, the t' phase could undergo spontaneous tetragonal-to-monoclinic transformation.[34] Since it is well-known in the martensite literature that substructures can impede martensitic growth, it is plausible that twin boundaries are the growth obstacles that render the t' phase seemingly untransformable. Together, these observations reinforce our impression that the t' phase and t phase differ only in their range of composition, and that they are fundamentally the same tetragonal phase in the zirconia solid solution.

V. Conclusions

The coexistence of the cubic fluorite and tetragonal phases in rapidly quenched samples has been explored in the ZrO_2–$MO_{1.5}$ systems for M = Sc, In, Y, and rare earths (R). The following conclusions are reached.

(1) Spontaneous transformation from metastable cubic phase to tetragonal phase can be triggered at room temperature by a mechanical force and the phase interface is sharp. Thus, the transformation is a martensitic one and is likely to be triggered by heterogeneous nucleation.

(2) Isolated tetragonal platelets in the cubic matrix are bounded by {101} habit planes. They also contain anti-phase boundaries. Mechanical twinning may follow the transformation to give rise to a multiply-twinned microstructure commonly associated with the so-called c-to-t' transformation reported in the literature.

(3) The tetragonality decreases with stabilizer content and vanishes around 18 mol% for M = Y and R, 23 mol% for M = Sc, and 25 mol% for M = In, all at room temperature. Thus, $ScO_{1.5}$ and $InO_{1.5}$ apparently have a different stabilizing effect from that of rare-earth oxides or yttria in the zirconia solid solutions.

(4) With increasing temperature, the tetragonality initially increases because of anisotropic thermal expansion, reaching a maximum before it decreases again as the equilibrium temperature for the tetragonal-to-cubic transformation is approached. As discontinuous change of tetragonality and a hysteresis loop accompany the transformation as the temperature or composition passes through the equilibrium value.

(5) The t' and t phases are fundamentally the same tetragonal polymorph in the zirconia solid solutions.

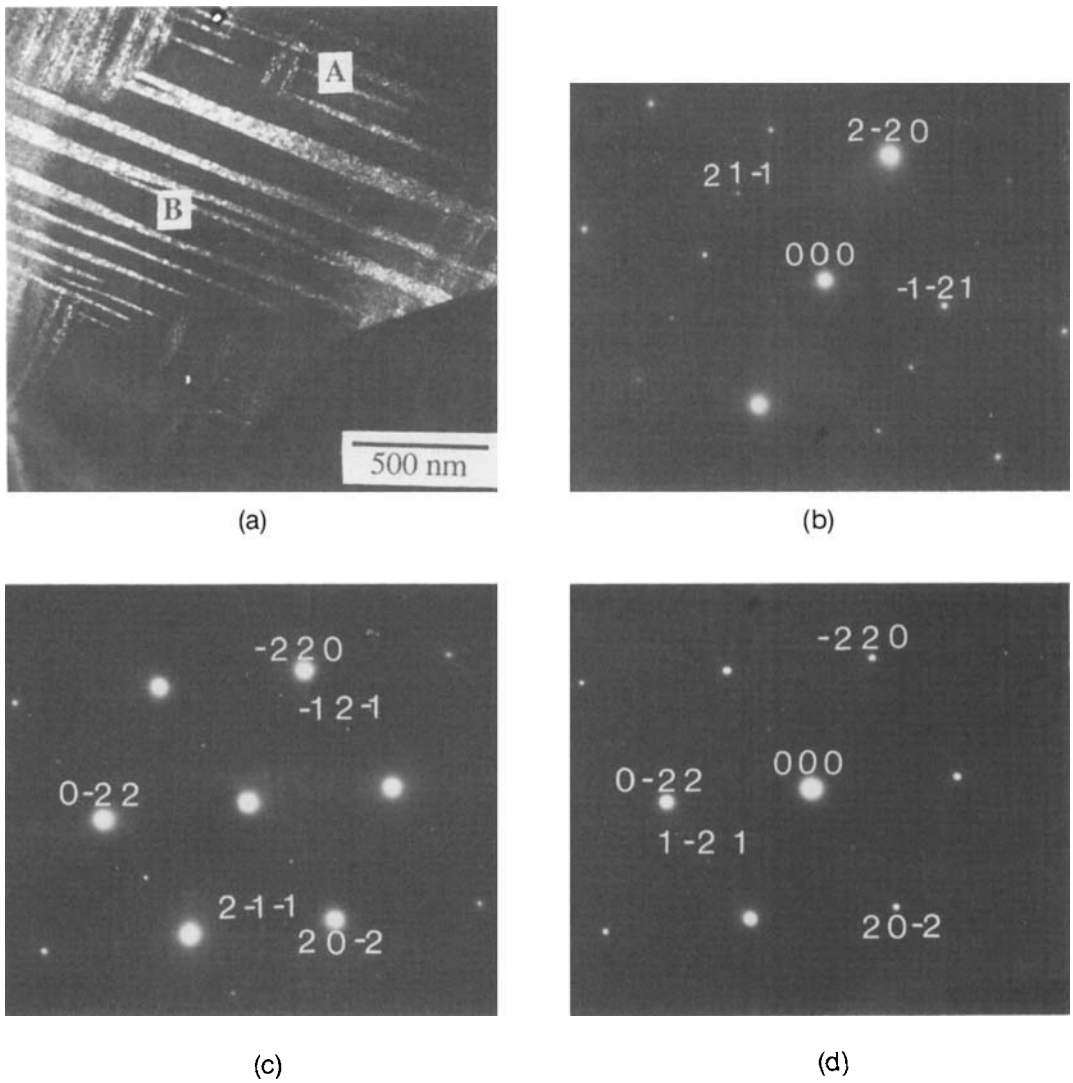

Fig. A2. A 14.4 mol% $YO_{1.5}$ sample containing several variants of t' phase inside the grain: (a) dark-field image from {112}, zone axis is [113]; (b) diffraction pattern, zone axis is [113]; (c) diffraction pattern from region A, zone axis is [111]; (d) diffraction pattern from region B, zone axis is [111].

APPENDIX

Further TEM Verification of the Coexistence of *c* and *t'* Phases

The coexistence of *c* and *t'* phases was also found in a sample containing 14.4 mol% $YO_{1.5}$. The TEM micrograph in Fig. A1 shows the *t'* plates emanating from the grain boundary and terminating inside the grain. Grains containing more than one variant of the *t'* phase, while still maintaining a cubic matrix, were also found as shown in the TEM micrograph of Figs. A2(a), which is a dark-field image using {112} reflection along the [113] zone axis. The diffraction patterns in Fig. A2(b) reveal two variants, both visible in Fig. A2(a) along with their characteristic APB. To further verify that there are no other tetragonal variants, we followed a procedure used by Heuer and co-workers.[5,12] Noting that all three variants in the *t'* phase could be imaged through ⟨112⟩ reflections with [111] zone axis, we tilted the sample to this zone axis and took selected area diffraction patterns from region A (which contains two variants) and region B (which contains one variant) of Fig. A2(a). In region A, shown in Fig. A2(c), we found only two sets of ⟨112⟩ reflections, one being weaker than the other. This indicates that there are two variants of the *t'* phase in region A, and one is dominating. In region B, shown in Fig. A2(d), we found essentially only one set of ⟨112⟩ reflections, with the other two nearly invisible. This indicates that one variant exists in region B. These observations are in obvious agreement with the dark-field image of Fig. A2(a), and leave no doubt that the matrix is not tetragonal. In other words, the *t'* variant is embedded in a cubic matrix.

References

[1]H. G. Scott, "Phase Relationships in the Zirconia–Yttria System," *J. Mater. Sci.*, **10** [9] 1527–35 (1975).

[2]R. A. Miller, J. L. Smialek, and R. G. Garlick, "Phase Stability in Plasma-Sprayed, Partially Stabilized Zirconia–Yttria"; pp. 241–55 in Advances in Ceramics, Vol. 3, *Science and Technology of Zirconia*. Edited by A. H. Heuer and L.W. Hobbs. American Ceramic Society, Columbus, OH, 1981.

[3]D. Michel, L. Mazeroles, M. Perez, and Y. Jorba, "Fracture of Metastable Tetragonal ZrO_2 Crystals," *J. Mater. Sci.*, **18**, 2618 (1983).

[4]A. H. Heuer and M. Rühle, "Phase Transformations in ZrO_2-Containing Ceramics I: The Instability of *c*-ZrO_2 and the Resulting Diffusion-Controlled Reactions"; pp. 1–13 in Advances in Ceramics, Vol. 12, *Science and Technology of Zirconia II*. Edited by N. Claussen, M. Rühle, and A. H. Heuer. American Ceramic Society, Columbus, OH, 1984.

[5]V. Lanteri, A. H. Heuer, and T. E. Mitchell, "The Tetragonal Phase in the ZrO_2–Y_2O_3 System"; pp. 118–30 in Advances in Ceramics, Vol. 12, *Science and Technology of Zirconia II*. Edited by N. Claussen, M. Rühle, and A. H. Heuer. American Ceramic Society, Columbus, OH, 1984.

[6]C. A. Anderson, J. Greggi, Jr., and T. K. Gupta, "Diffusionless Transformation ZrO_2 Alloys"; pp. 118–30 in Advances in Ceramics, Vol. 12, *Science and Technology of Zirconia II*. Edited by N. Claussen, M. Rühle, and A. H. Heuer. American Ceramic Society, Columbus, OH, 1984.

[7]B. Bender, R.W. Rice, and J. K. Spann, "Precipitate Character in Laser-Melted PSZ," *J. Mater. Sci. Lett.*, **4**, 1331–36 (1985).

[8]R. Chaim, M. Rühle, and A. H. Heuer, "Microstructural Evolution in a ZrO_2–12 wt% Y_2O_3 Ceramic," *J. Am. Ceram. Soc.*, **68** [8] 427–31 (1985).

[9]T. Sakuma, Y.-I. Yoshizawa, and H. Suto, "The Microstructure and Mechanical Properties of Yttria-Stabilized Zirconia Prepared by Arc-Melting," *J. Mater. Sci.*, **20** [10] 2399–407 (1985).

[10]V. Lanteri, R. Chaim, and A. H. Heuer, "On the Microstructure Resulting from the Diffusionless Cubic → Tetragonal Transformation in ZrO_2–Y_2O_3 Alloys," *J. Am. Ceram. Soc.*, **69** [109] C-258–C-261 (1981).

[11]R. Chaim, V. Lanteri, and A. H. Heuer, "The Displacive Cubic → Tetragonal Transformation in ZrO_2 Alloys," *Acta Metall.*, **35** [3] 661–66 (1984).

[12]A. H. Heuer, R. Chaim, and V. Lanteri, "Review: Phase Transformations and Microstructural Characterization of Alloys in the System Y_2O_3–ZrO_2"; pp. 3–20 in Advances in Ceramics, Vol. 24A, *Science and Technology of Zirconia III*. Edited by Sōmiya, N. Yamamoto, and H. Yanagida. American Ceramic Society, Westerville, OH, 1988.

[13]M. Yoshimura, "Phase Stability of Zirconia," *Am. Ceram. Soc. Bull.* **67** [12] 1950–55 (1988).

[14]J. Lefevre, "Fluorite-type Structural Phase Modification in Systems Having a Zirconium or Hafnium Oxide Base," *Ann. Chim.*, **8** [1–2] 117–49 (1963); or translated by A. L. Monka, ORNL-TR-201.

[15]D. J. Kim, "The Effect of Alloying on the Transformability of Y_2O_3-Stabilized Tetragonal ZrO_2"; Doctoral Dissertation. Department of Materials Science and Engineering, University of Michigan, Ann Arbor, MI, 1988.

[16]L.V. Morozova *et al.*, "Electrical Properties of ZrO_2–In_2O_3 Solid Solutions," *Russ. J. Phys. Chem. (Engl. Transl.)*, **60** [6] 853–55 (1986).

[17]F. M. Spiridonov, L. N. Popova, and R. Ya. Popil'skii, "On the Phase Relations and the Electrical Conductivity in the System ZrO_2–Sc_2O_3," *J. Solid State Chem.*, **2**, 430–38 (1970).

[18]T. Sakuma and H. Soto, "Cubic–Tetragonal Phase Separations in Y-PSZ"; pp. 531–35 in Advances in Ceramics, Vol. 24A, *Science and Technology of Zirconia III*. Edited by S. Sōmiya, N. Yamamoto, and H. Yanagida. American Ceramic Society, Westerville, OH, 1988.

[19]M. S. Wechsler, D. S. Lieberman, and T. A. Read, "On the Theory of the Formation of Martensite," *Trans. AIME*, **197** [November] 1503–15 (1953).

[20]M. Shibata-Yanagisawa, M. Kato, H. Seto, N. Ishizawa, N. Mizutani, and M. Kato, "Crystallographic Analysis of the Cubic-to-Tetragonal Phase Transformation in the ZrO_2–Y_2O_3 System," *J. Am. Ceram. Soc.*, **70** [7] 503–509 (1987).

[21]J. S. Bowles, C. S. Barrett, and L. Guttman, "Crystallography of Cubic–Tetragonal Transformation in the Indium–Thallium System," *J. Met.*, **188** [December] 1478–85 (1950).

[22]M. Kato, M. Shibata-Yanagisawa, and H. Seto, "Reply on Crystallographic Analysis of the Cubic-to-Tetragonal Phase Transformation in the ZrO_2–Y_2O_3 System," *J. Am. Ceram. Soc.*, **71** [3] C-171–C-172 (1988).

[23]I-W. Chen and Y. H. Chiao, "Theory of Martensitic Nucleation in Zirconia-Containing Ceramics," *Acta Metall.*, **33** [10] 1827–45 (1985).

[24]Y.-H. Chiao and I-W. Chen, "Martensitic Growth in ZrO_2—An In-situ, Small Particle, TEM Study of a Single Interface Transformation," *Acta Metall.*, **38** [6] 1163–74 (1990).

[25]P. Alderbert and J. P. Traverse, "Structure and Ionic Mobility of Zirconia at High Temperature," *J. Am. Ceram. Soc.*, **68** [1] 34–40 (1985).

[26]K. Negita, "Lattice Vibrations and Cubic to Tetragonal Phase Transition in ZrO_2," *Acta Metall.*, **37** [1] 313–17 (1989).

[27]L. Landau and E. Lifshitz, *Statistical Physics*. Pergamon Press, New York, 1958.

[28]F. Jona and G. Shirane, *Ferroelectric Crystals*. Pergamon Press, New York, 1962.

[29]G. B. Olson and M. Cohen, "Classical and Nonclassical Mechanisms of Martensitic Transformation," *J. Phys.*, **43** [12] Supplement, C4-75–88 (1982).

[30]G. B. Olson and M. Cohen, "Theory of Martensitic Nucleation, A Current Assessment"; pp. 1145–64 in Proceedings of an International Conference on Solid–Solid Phase Transformations, Carnegie-Mellon University, Pittsburgh, PA, August 10–14, 1981. Edited by H. Aaronson. American Institute of Mining, Metallurgical and Petroleum Engineers, New York, 1982.

[31]G. B. Olson, "Lattice Stability and the Mechanism of Martensitic Transformation"; pp. 25–34 in Proceedings of an International Conference on Martensitic Transformation. Japan Institute of Metals, Tokyo, Japan, 1986.

[32]S. M. Ho, "On the Structural Chemistry of Zirconium Oxide," *Mater. Sci. Eng.*, **54**, 23–29 (1982).

[33]T-S. Sheu, "Phase Stability of Zirconia Solid Solutions"; Doctoral Dissertation. Department of Materials Science and Engineering, University of Michigan, Ann Arbor, MI, 1989.

[34]J. F. Jue, J. Chen, and A.V. Virkar, "Low Temperature Aging of *t'*-Zirconia: The Role of Microstructure on Phase Stability," *J. Am. Ceram. Soc.*, **74** [8] 1811–20 (1991). □